Water Channels

DOI: 10.1002/anie.201103312

Imidazole-Quartet Water and Proton Dipolar Channels**

*Yann Le Duc, Mathieu Michau, Arnaud Gilles, Valerie Gence, Yves-Marie Legrand, Arie van der Lee, Sophie Tingry, and Mihail Barboiu**

Most vital physiological processes depend on unique exchanges of particles between a cell and its environment.[1] Gramicidin,[2] KCsA K^+,[3] aquaporin,[4] and influenza A virus M2[5] channels are well known, nonexclusive examples of proteins in which ions, water molecules, and protons are envisioned to diffuse along water-filled pores.[1–5]

Powerful synthetic scaffolds mimicking natural protein functions unlock the door to a world of interactive materials paralleling that of biology. Numerous artificial systems showing a rich array of interconverting ion-channel conductance states in phospholipid and polymeric membranes have been developed in the last decades.[6–9] However, there has been less progress in the area of synthetic water channels. Among different water clusters,[10] one-dimensional water wires have attracted much interest. Sophisticated structures[11,12] have been designed to mimic natural aquaporin water[4,13] and influenza A M2 proton channels.[5] Hydrophobic[1b,11] and hydrophilic[12] pores have been designed to selectively transport water against ions. Such molecular-scale hydrodynamics[14] of water through the channel will depend on channel–water and water–water interactions, as well as on the electrostatic dipolar profile of the water in the channel.[13] On the same principle, proton selectivity, and low-pH gating are key functions of influenza A M2 proton channel. Although there is some variability in setting off the proton/water-transport mechanisms, many structural features are related to imidazole quartet (I-quartet), implicated in the $(His^{37})_4$ selectivity filter (Figure 1).[5] Despite a wealth of experimental data major issues need to be resolved at the atomic level. Moreover such artificial biomimetic systems are of great interest for the design of dynamic interactive systems for molecular information transfer.[9]

Artificial tubular architectures of self-assembled imidazole units, mutually stabilized by strong H-bonding with inner water molecules, are excellent candidates as functional water(proton)-channel systems.[12a–c] Moreover, we and others previously showed that urea ribbons are very useful to design artificial ion-channel systems.[7]

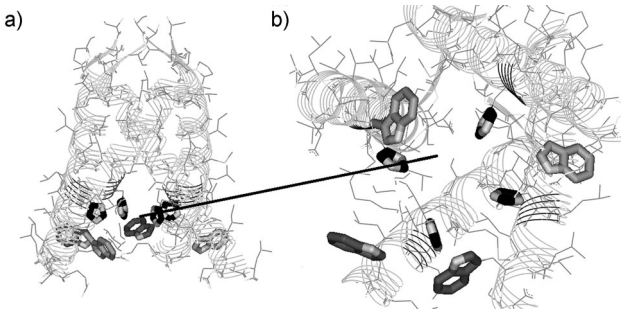

Figure 1. a) Side and b) C-terminal crystal structure (3PKD.pdb, 3pKD.cif) of His/Trp gate of influenza A virus M2 proton channel: $(His^{37})_4$ (black sticks) and $(Trp^{41})_4$ (gray sticks) quartets are strongly involved in proton gating.[5]

In this study, ureido imidazole compounds were used as molecular scaffolds to construct I-quartets, mutually stabilized by inner water wires in a manner reminiscent of that by which G-quartets are stabilized by cation templating.[8] Ureido imidazole monomers **1** and **2** (Scheme 1a) were designed to place the urea and imidazole groups in a spatially separated configuration. They form I-quartet tubular architectures including water-wire arrays in the solid state and show water-channel conductance states in bilayer membranes. From the mechanistic point of view, we start with molecular components which can self-assemble into oligomeric I-quartets, and exhibit potential membrane-spanning water-channel behavior at the supramolecular level.

Hexyl isocyanate and hexyl diisocyanate were treated with the corresponding amount of histamine (CH_3CN/*N*,*N*-dimethylacetamide, 120 °C, 5 h) to afford after crystallization **1** and **2**, respectively, as white powders. The ^1H and ^{13}C NMR and ESI-MS spectra of **1** and **2** are in agreement with the proposed formulas (see Supporting Information). Colorless single crystals of **1** and **2** were obtained by recrystallization from water at room temperature. The structures of **1** and **2** reveal the expected ureido imidazole compounds, and the unit cell contains four molecules of **1** and eight molecules of **2**, respectively, together with four molecules of water. The crystal structures of **1** and **2** reveal homomeric association (urea–urea and imidazole–imidazole/imidazole–water) of H-bonding sites (Scheme 1b).[12c] In the solid state, the neighboring urea units lie in the exact same plane and thus impose a planar conformation on the urea ribbon. The NH···O=C H-bonds lengths ($d_{O\cdots H} = 2.00$, 2.13 Å) are the same along the ribbon and are consistent with other urea systems.[7]

Each molecule of **1** is stretched to its maximum theoretical length (> 26.9 Å, Figure 2a). Two conformers of **2** are present in the solid state: elongated (18.3 Å) and contracted (16.7 Å)

[*] Dr. Y. Le Duc, Dr. M. Michau, Dr. A. Gilles, V. Gence, Dr. Y.-M. Legrand, Dr. A. van der Lee, Dr. S. Tingry, Dr. M. Barboiu
Adaptative Supramolecular Nanosystems
Institut Européen des Membranes – UMR CNRS
5635, Place Eugène Bataillon, CC 047, 34095 Montpellier (France)
E-mail: barboiu@iemm.univ-montp2.fr

[**] This work was supported by funds from ANR ANR 2010 BLAN 7172 and EURYI 2004 (European Young Investigator Awards scheme; see www.esf.org/euryi)

Supporting information for this article is available on the WWW under http://dx.doi.org/10.1002/anie.201103312.

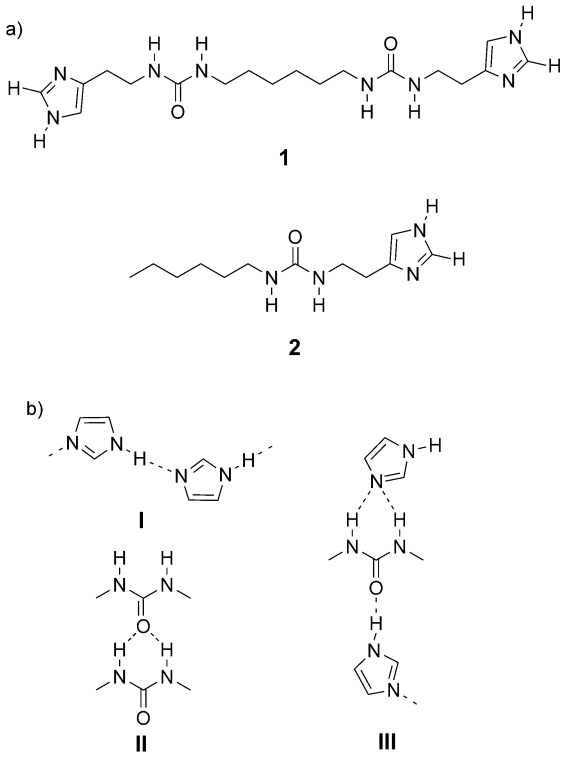

Scheme 1. a) Structure of synthesized ureido imidazole compounds **1**, **2**. b) Homomeric (I, II) and heteromeric (III) associations of imidazole and of urea H-bonding units.

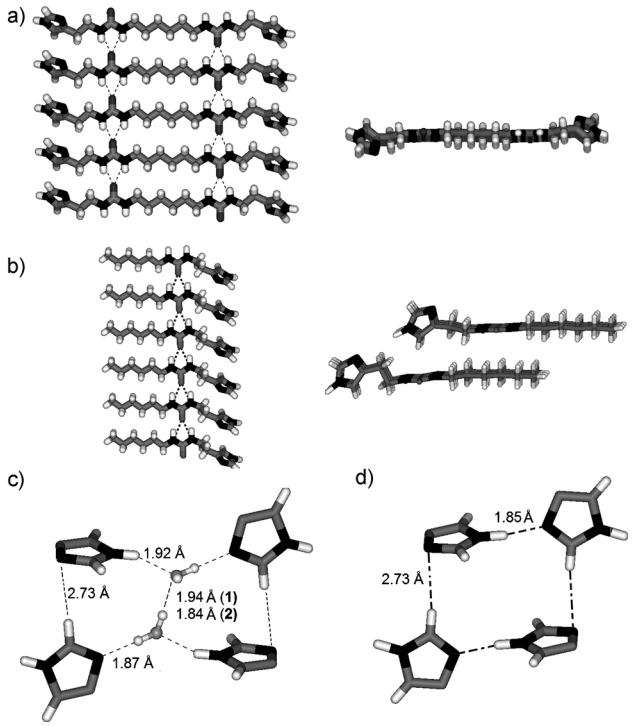

Figure 2. Solid-state structures of a) **1** and b) **2**: side and top views in stick representation (N, black, C, gray, O, light gray, H white) of continual planar arrays of the H-bonded urea ribbons. c) Water-assisted formation of I-quartet "open form" through CH···N and NH···O H-bond interactions. Water molecules in ball-and-stick representation are H-bonded through OH···O interactions. d) Formation of I-quartet "off form" through CH···N and NH···N H-bond interactions in the absence of water.

geometries are dependent on the nature of the H-bonds involving the terminal imidazole groups in the crystal (Figure 2b). Accordingly, continual planar arrays of layered stacks of **1** and **2** are generated in the solid state, such that the imidazole moieties are disposed at the extremities of each ribbon. They are involved in interesting interlayer interactions corresponding to 1) water assisted I-quartet formation via CH···N, N···HO, and NH···O-H interactions (Figure 2c) and 2) water-free I-quartet formation via CH···N and NH···N interactions (Figure 2d). Weak π–π stacking interactions between imidazole moieties of two neighboring molecules of **1** ors **2** and strong hydrophobic van der Waals interaction between the hexyl chains stabilize the ribbonlike superstructures (Figure 2 and Figure 1S, Supporting Information).

The water molecules in **1** form strong H-bonds with imidazole nitrogen atoms. One 100% occupancy H atom is bonded to imidazole N, while the other H atom is 50% disordered over two positions, as previously observed.[12a] Two 50% H atoms are H-bonded to neighboring water molecules, defining zigzag wires[15] in which the water molecules are crystallographically restricted to two orientations in a such way that all water molecules of one channel have the same dipolar orientation. Water molecules are alternately oriented in opposite directions into neighboring channels (Figure 3a). Compound **2** has a different packing that results in alternative I-quartet water channels, separated by water-free I-quartets, and the overall structure has an inversion center (Figure 3b). Thus, water channels of opposite dipolar orientation are present in successive channels, whereby both H atoms of the water molecules show 100% occupancy. The oxygen atom of each water molecule in **1** and **2** is simultaneously strongly H-bonded to both imidazole NH groups ($d_{O\cdots H} = 1.93$ Å) and the vicinal water molecules ($d_{O\cdots H} = 1.94$ Å in **1** and 1.84 Å in **2**). Water molecules form a more compact wire motif in **2** than in **1**. The I-quartet water channels of rhomboidal shape (4.9×4.1 Å^2 for **1** and 4.4×4.0 Å^2 for **2**, considering a projection on a plane and not taking into account the van der Waals radii of diagonally located N and CH sites) determine a gap in the channel of 2.6 Å, very close to narrowest constriction observed in aquaporin water channels (2.8 Å).[13]

Motional disorder of water molecules has been probed by static and MAS ^{2}H NMR spectroscopy.[12a,b] Considering the electron density map of water molecules, we may argue that both crystal structures of **1** or **2** are not really associated with local water disorder/motion (Figures 2S and 3S, Supporting Information). These assumptions were confirmed by thermal analysis. In contrast to previous water-channel superstructures,[12a,b,e] thermogravimetric analysis showed that synergetic water loss and decomposition of the matrix of **1** and **2** occur over a large temperature range of 200–300 °C, reminiscent of a strong water binding within the channels. The differential scanning calorimetric (DSC) data are consistent with single sharp endotherms centered at 200.1 °C for **1** (Figure 4S, Supporting Information) and 132.4 °C for **2** (Figure 5S, Supporting Information). The overall change in enthalpy

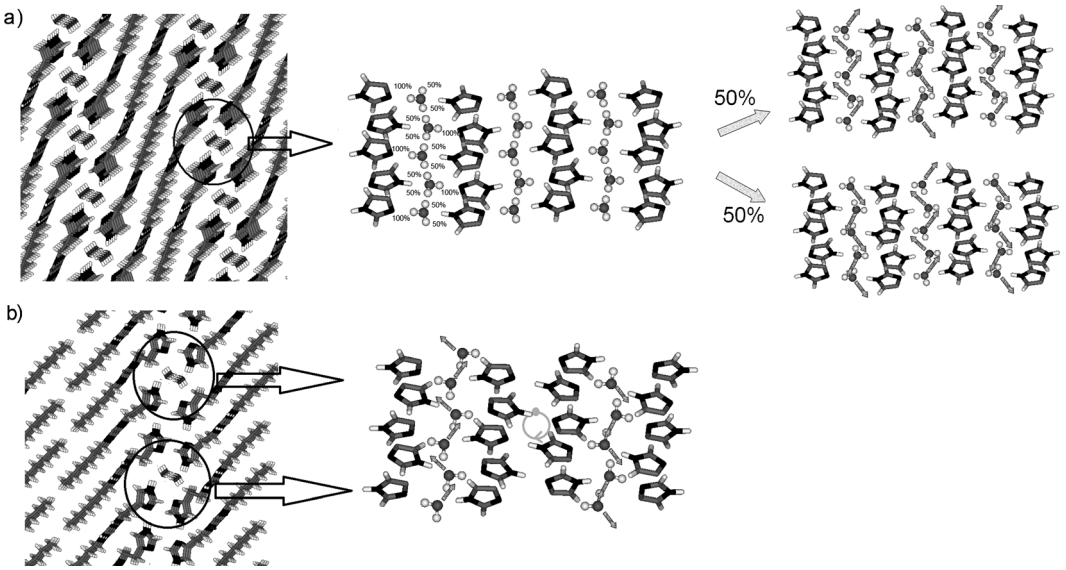

Figure 3. Crystal packing of a) **1** and b) **2**: side and top views in stick representation (N, black, C, gray, O, light gray, H white) of continual planar arrays of layered-type stacks generating channels of water molecules of unique dipolar orientation (see text for details). Water molecules in ball-and-stick representation.

per water molecule is 21.8 kcal mol^{-1} for **1** and 24.9 kcal mol^{-1} for **2**, consistent with strong cooperativity of water binding within the channel superstructure. These values agree with N···H-O and NH···OH bond lengths observed in X-ray crystal structures, which are about 1 Å shorter than theoretical values reported for imidazole–water pairs in aqueous solution.[17] The DSC plot of monosubstituted compound **2** shows also a glass transition centered at 83.9 °C, consistent with thermal denaturation of the hydrophobic interface between the hexyl chains.

Water transport across bilayer membranes incorporating **1** and **2** I-quartets was assessed by dynamic light scattering (DLS) by using a modification of a previously described method.[18] The osmotic behavior of unilamellar EYPL (3-*sn*-phosphatidylcholine) liposomes containing NaCl entrapped inside the vesicles and suspended in pure water causes water influx into vesicles. The decrease in light scattering (number of counts at 600 nm) caused by vesicle swelling and then destruction is related to the increasing permeability of the water bilayer due to formation of I-quartet water channels by compounds **1** and **2**. Aliquots of DMSO solutions of **1** and **2** (0–40 mM) were injected into unilamellar liposomes in which a stable bilayer membrane had formed. Both compounds elicited a low level of membrane disruption within minutes of exposure to 10 mM of compound. Significant membrane disruption was observed on injection of aliquots of the more concentrated solutions (Figure 4).

Figure 4 shows that high water-transport activity ($k = 1.2 \times 10^{-3}$ min^{-1}) is obtained when **1** or **2** is present, compared with the control measurements in which only DMSO was added to liposomes ($k = 8.7 \times 10^{-5}$ min^{-1}). The channels in this region could be viewed as derived from the crystal structure of **1** and **2**, in which tubular I-quartet oligomers would probably form a barreled channel (see Figure 4c). The real transporting structure within bilayer membrane may be composed of successive I-quartet "open-form" and "off-form" configurations (Figure 2c, d), avoiding disruption of conductive functional states. The increased levels of water conductance observed for these species at higher concentration would then be interpreted as multiple copies of the transmembrane barreled channels starting at a critical concentration of 10 mM. The formation of conductive architectures is probably related to their robustness, given that their aggregation correlates to transport properties: 1) the rigid bis-ureido imidazole **1** showed an exponential behavior needing a larger critical amount of I-quartet to be present within the bilayer; b) the more labile mono-ureido imidazole can generate a cooperative replication of the conductive I-quartet systems within the bilayer showing a sigmoid $k = f(t)$ profile. This confirms that better organization (closer packing) in the monolayer correlates to poorer water transport.

Furthermore, no measurable transport of Li^+ and Na^+ cations was observed through monitoring changes in fluorescence intensity ratio with vesicle internal pH by a pH-gradient method previously used by Davis and co-workers (Figure 6S, Supporting Information).[8c] The diameters of Li^+ (3.1 Å) and Na^+ (3.6 Å) cations with their hydration shells are greater than the narrowest channel diameter (2.6 Å) and would require partial dehydration for pore passage, which would lead to unfavorable interactions with the different N sites of the channel.[19] Similar ion-exclusion phenomena have been reported for carbon nanotube systems.[20] The same results were obtained when unilamellar EYPL liposomes containing NaCl entrapped inside the vesicles were suspended in Na_2SO_4 solution (Figures 7Sa and 8Sa, Supporting Information). Over a number of experiments such systems operating under non-osmotic pressure are inactive to transport of water, ions, or protons. With this in mind, the osmotic unilamellar EYPL liposomes containing NaCl and the acid dye 8-hydroxypyrene-1,3,6-trisulfonate (HPTS) entrapped inside the vesicles

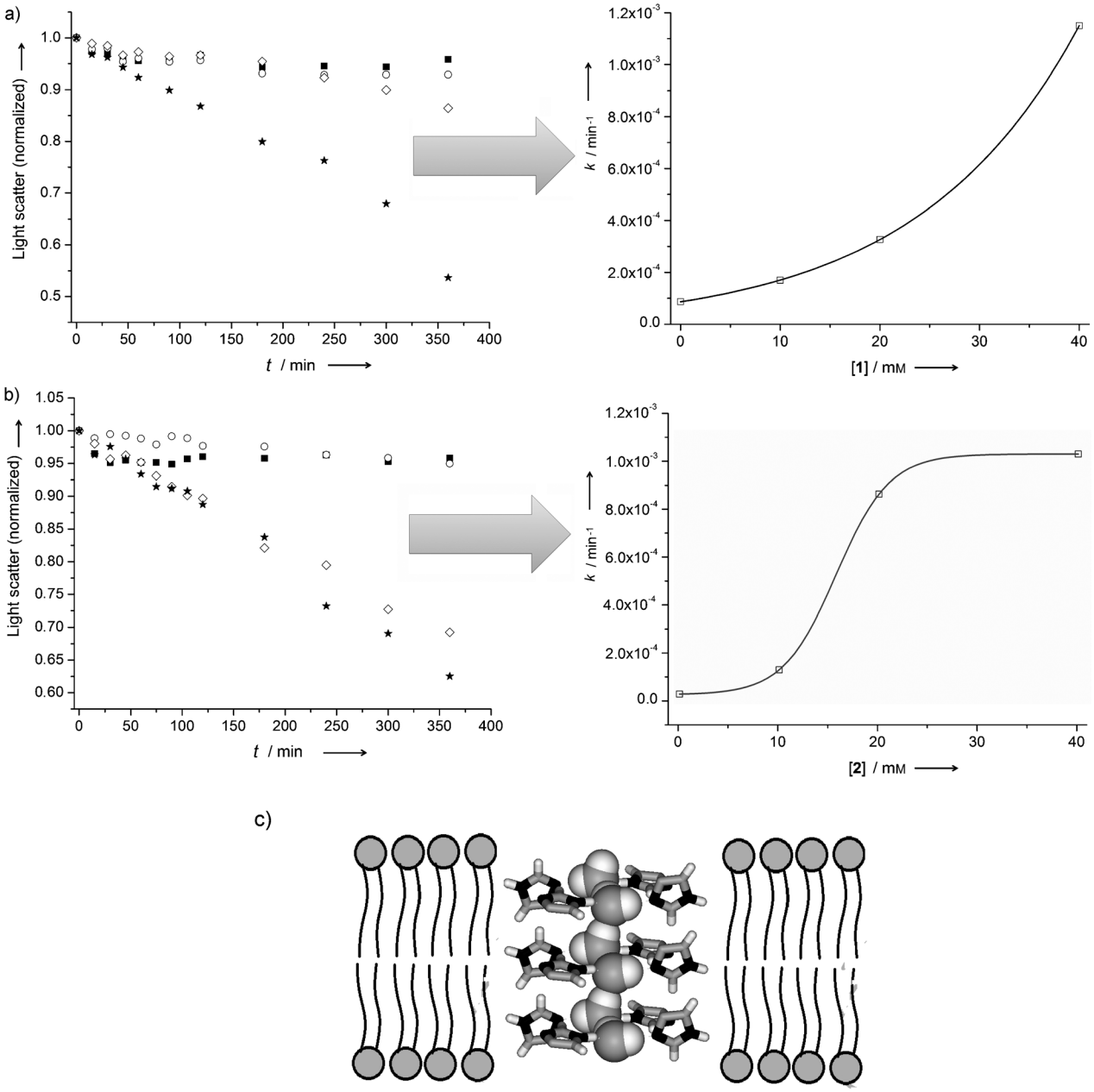

Figure 4. Decrease in light scattering in DMSO (■) and with 10 (○), 20 (◇), and 40 mM (★) DMSO solutions of a) **1** and b) **2** I-quartet systems. The collected data were normalized to fit between 0 and 1. Right insets: Exponential rise of rate constants *k* with compound concentration. Rate constants were determined by curve fitting of the plots to a single-order exponential.[18] c) Schematic of possible organization of components in a barreled model within a bilayer membrane.

were suspended in pure water and tested by the fluorescence method without pH gradient. The influx water transport shown by DLS experiments equally determines quenching of the fluorescence of HPTS; this supports the assumption that the water channels are involved in proton transport across the membrane toward the extravesicular solution, which probably occurs with co-transport of chloride anions to the exterior of the vesicles. The osmotic swelling causes vesicles to grow and alters the ionic balance between the lipids, which may be compensated by the absorption of ion pairs of protonated imidazole molecules accepting the proton of HPTS molecules. However, the proton-transport activity of the I-quartet systems over a 10–40 mM concentration domain (Figure 5) shows the sequence **2** > **1**. Transport of protons along water wires of monodipolar orientation may occur through a Grothuss mechanism.[21] The oxygen–oxygen distance of $r_{OO} = 2.60$ Å for an ideal Eigen cation is comparable with distances of 2.75–2.80 Å observed in the crystal structures of **1** and **2**.[21b] Strong translational and orientational control of water molecules, involving much stronger dipole conservation along the channel, can explain the higher proton transport rate of **2** compared to **1**, as a result of stabilization of

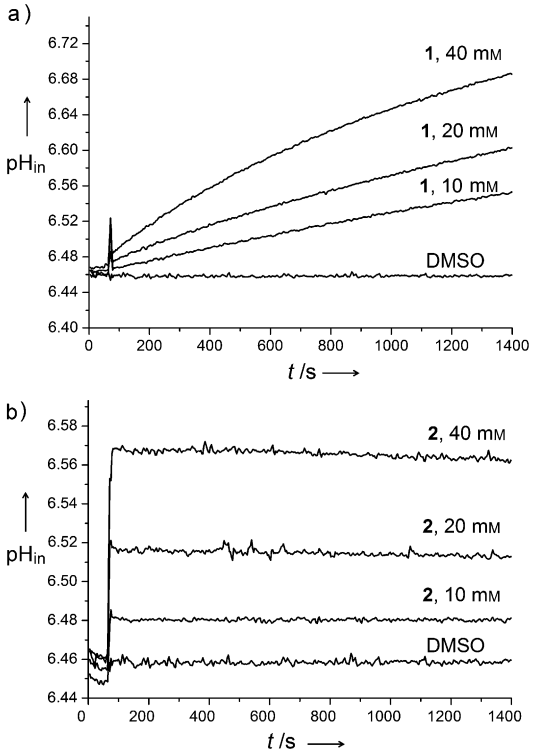

Figure 5. Transport of protons as determined in an osmotic gradient assay. EYPL liposomes (100 nm) containing HPTS dye (0.1 mM) in 100 mM NaCl and 10 mM sodium phosphate (pH 6.4) were suspended in pure water. Compounds **1** (a) and **2** (b) were added at $t = 60$ s The background experiment was performed with pure DMSO solvent. Measurement of the ratiometric fluorescence intensity of HPTS ($\lambda_{ex,1} = 403$, $\lambda_{ex,2} = 460$, $\lambda_{em} = 510$ nm) allowed determination of the internal liposomal pH_{in} (see Experimental and Supporting Information for details).

the water wires. They are more compact (Figure 2c, d) and structurally adapted to channel macrodipoles within the channels of **2** compared with **1**, as observed in their crystal structures.

In conclusion, we have used ureido imidazoles **1** and **2** to construct I-quartets mutually stabilized by inner water dipolar wires, reminiscent of G-quartets stabilized by cation templating.[8,9] The H-bonding of these I-quartets leads to tubular solid-state structures and, in a membrane environment, to a barreled channel. The encapsulated water molecules, like in aquaporin water channels, form one H-bond with the inner wall of the I-quartet nanotube and one with an adjacent water molecule.[13] Within the I-quartet nanotubes water molecules of unique dipolar orientation can preserve the electrochemical potential along the channel. Our results strongly indicate that water molecules and protons can permeate bilayer membranes through I-quartet channels. Strong interactions of the water with the inner surface of the I-quartet nanotube reduce the efficiency of water transport compared to the aquaporin system. In contrast to aquaporin systems,[13,18] the water wires preserve a unique dipolar orientation, and I-quartet systems are good candidates for proton translocation, while cations are excluded. The ion-exclusion phenomena are based on dimensional steric effects, whereas hydrophobic[11d] and hydrodynamic[20] effects appear to be less important. Water-free I-quartet "off form" superstructure (Figure 1d) is reminiscent of the closed conformation of the His^{37}-quartet system[5] of the proton gate of influenza A M2 protein. The slight conformational adjustments allow formation of the water-assisted I-quartet "open form" (Figure 1c), through which protons can diffuse along dipolar oriented water wires in the open-state pore-gate region. These artificial I-quartet superstructures obtained by using simple chemistry are in excellent agreement with structural X-ray and NMR results as well as theoretical results providing accurate structural information for water/proton conductance mechanisms through an influenza A M2 proton channel. However, it was shown that Trp^{41} residues in close proximity of the His^{37} quartet exclude water molecules from the gating region due to steric effects, and only highly protonated His models show a conductance state through the channel. Further studies including His-Trp systems to prove this hypothesis are in progress.

Experimental Section

Crystal data: X-Ray Crystallographic data for **1** were recorded with an Xcalibur CCD camera (Oxford Diffraction) using graphite-monochromated $Mo_{K\alpha}$ radiation ($\lambda = 0.71073$ Å), 28 s per frame. Structure **1** was solved by direct methods with SHELX86, and structure **2** with SIR2002.[22a] The two structures were refined by least-squares methods on F by using CRYSTALS[22b] against $|F|$ on data having $I > 2\sigma(I)$; R factors are based on these data. Hydrogen atoms were partly located from difference Fourier synthesis, partly placed on the basis of geometrical arguments, and refined. Non-hydrogen atoms were refined anisotropically. Hydrogen atoms were located from the Fourier difference map and refined with riding constraints. CCDC 830733 and 830734 contain the supplementary crystallographic data for this paper. These data can be obtained free of charge from The Cambridge Crystallographic Data Centre via www.ccdc.cam.ac.uk/data_request/cif.

Crystal data for **1**: $C_{18}H_{34}N_8O_4$, $M_r = 426.53$, monoclinic, space group $P21/c$, $a = 14.5480(9)$, $b = 4.5839(3)$, $c = 16.8540(10)$ Å, $\beta = 100.471(6)°$, $V = 1104.89(14)$ Å^3, $Z = 4$, $\rho_{calcd} = 1.279$ g cm^{-3}, $T = 173$ K, $\mu(0.51091\ \text{Å}) = 0.100$ mm^{-1}, 9126 reflns collected, 1738 unique reflns with $I > 2\sigma(I)$, $R_F = 0.1073$ and $wR_F = 0.0731$ for all reflns, $R_F = 0.0696$ and $wR_F = 0.0690$ for observed reflections.

Crystal data for **2**: $C_{24}H_{46}N_8O_3$, $M_r = 494.68$, monoclinic, space group $P21/c$, $a = 27.671(3)$, $b = 4.5892(3)$, $c = 23.954(2)$ Å, $\beta = 113.354(13)°$, $V = 2792.6(6)$ Å^3, $Z = 4$, $\rho_{calcd} = 1.439$ g cm^{-3}, $T = 173$ K, $\mu(0.51091\ \text{Å}) = 0.100$ mm^{-1}, 4331 reflns collected, 3357 unique reflns $I > 2\sigma$ (I), $R_F = 0.0776$ and $wR_F = 0.0728$ for all reflns, $R_F = 0.0599$ and $wR_F = 0.0584$ for observed reflections.

Preparation of EYPL (3-*sn*-phosphatidylcholine) unilamellar vesicles: Egg yolk L-α-phosphatidylcholine (EYPC in $CHCl_3$, 600 μL, 790 μmol) was dissolved in $CHCl_3$/MeOH, the solution was evaporated under reduced pressure, and the resulting thin film was dried under high vacuum for 2 h. The lipid film was hydrated for 40 min in 1.2 mL of phosphate buffer (10 mM sodium phosphate, pH 6.4, 100 mM NaCl) containing 10 μM HPTS. During hydration, the suspension was subjected to five freeze–thaw cycles (liquid nitrogen, water at room temperature). The suspension of large multilamellar liposomes (1 mL) was subjected to high-pressure extrusion at room temperature (21 extrusions through a 0.1 μm polycarbonate membrane afforded a suspension of large unilamellar liposomes (LUVs) with an average diameter of 100 nm). The LUV suspension was separated from extravesicular dye by size-exclusion chromatography (stationary phase: Sephadex G-50, mobile phase: phosphate buffer)

and diluted with the same phosphate buffer to give a stock solution with a lipid concentration of 11 mM (assuming 100% of lipid was incorporated into liposomes). Vesicles prepared in this manner were analyzed by DLS, which showed a highly homogenous vesicular solution with vesicle diameter of 94.5–100 nm (Figure 9S, Supporting Information)

Water-transport experiments: Water permeability was determined by DLS on a Zetasizer Nano Serie S apparatus from Malvern. 100 μL of vesicle stock solution containing 10 mM of sodium phosphate buffer (pH 6.4) and 100 mM of sodium chloride was diluted in 1.9 mL of distilled water and stirred. 20 μL of a DMSO solution containing different concentrations of **1** or **2** was added to cause water influx into vesicles. The decrease in light scattering (number of counts) caused by vesicle swelling and then destruction were recorded under the following experimental conditions: $t = 25\,^{\circ}C$, position: 4.65 mm, attenuator: 6, dispersant: water; refractive index (R.I.): 1.33; viscosity: 0.887, recording time: 60 s; material R.I.: 1.59. Results were normalized to fit between zero and unity, and rate constants were calculated by using a linear fit model by subtracting the DMSO baseline observed in control experiments.

Proton-transport experiments: 100 μL of HPTS-loaded vesicles (stock solution) was suspended in 1.9 mL of milliQ water (osmotic gradient assay, Figures 7Sb and 8Sb of the Supporting Information) or 1.9 mL of sodium phosphate solution, pH 6.5 with 50 mM Na_2SO_4 (non-osmotic gradient assay, Figures 7Sb and 8Sb of the Supporting Information) and placed in a fluorimetric cell. The emission of HPTS at 510 nm was monitored with excitation wavelengths of 403 and 460 nm. During the experiment, 20 μL of a 0–40 mM DMSO solution of compound **1** or **2** was added at $t = 60$ s. Maximal possible changes in dye emission were obtained at $t = 500$ s by lysis of the liposomes with detergent (40 μL of 5% aqueous Triton X100). The pH values were calculated for each point from the HPTS emission intensities according to the calibration equation $pH = 1.1684\,lg(I_o/I_1) + 6.9807$, where I_o is the emission intensity with excitation at 460 nm, and I_1 the emission intensity with excitation at 403 nm. At the end of experiment, the aqueous compartment of the liposomes was equilibrated with extravesicular solution by lysis of liposomes with detergent (40 μL of 5% Triton X100).

Received: May 14, 2011
Published online: August 24, 2011

Keywords: hydrogen bonds · influenza A M2 channel · proton transport · supramolecular chemistry · water channels

[1] F. Hucho, C. Weise, *Angew. Chem.* **2001**, *113*, 3194 – 3211; *Angew. Chem. Int. Ed.* **2001**, *40*, 3100 – 3116.

[2] a) S. Cukiermann, *Biophys. J.* **2000**, *78*, 1825 – 1834; b) D. A. Dougherty, *Science* **1996**, *271*, 163 – 168; c) J. P. Gallivan, D. A. Dougherty, *Proc. Natl. Acad. Sci. USA* **1999**, *96*, 9459 – 9464.

[3] R. Mackinnon, *Angew. Chem.* **2004**, *116*, 4363 – 4376; *Angew. Chem. Int. Ed.* **2004**, *43*, 4265 – 4277.

[4] P. Agre, *Angew. Chem.* **2004**, *116*, 4377 – 4390; *Angew. Chem. Int. Ed.* **2004**, *43*, 4278 – 4290.

[5] a) J. R. Schnel, J. J. Chou, *Nature* **2008**, *451*, 591 – 595; b) A. L. Stouffer, R. Acharya, D. Salom, A. S. Levine, L. Di Constanzo, C. S. Soto, V. Tereshko, V. Nanda, S. Stayrook, W. F. DeGrado, *Nature* **2008**, *451*, 596 – 599; c) S. Phongphanphanee, T. Rungrotmongkol, N. Yoshida, S. Hannongbua, F. Hirata, *J. Am. Chem. Soc.* **2010**, *132*, 9782 – 9788; d) F. Hu, W. Luo, M. Hong, *Science* **2010**, *330*, 505 – 508; e) M. Sharma, M. Yi, H. Dong, H. Qin, E. Paterson, D. D. Busath, H.-X Zhou, T. A. Cross, *Science* **2010**, *330*, 509 – 511; f) L. H. Pinto, G. R. Dieckmann, C. S. Gandhi, C. R. Papworth, J. Braman, M. A. Saughnessy, J. D. Lear, R. A. Lamb, W. F. DeGrado, *Proc. Natl. Acad. Sci. USA* **1997**, *94*, 11301 – 11306.

[6] a) G. W. Gokel, A. Mukhopadhyay, *Chem. Soc. Rev.* **2001**, *30*, 274 – 286; b) N. Voyer, *Top. Curr. Chem.* **1996**, *184*, 1 – 35; c) D. T. Bong, T. D. Clark, J. R. Granja, M. R. Ghadiri, *Angew. Chem.* **2001**, *113*, 1016 – 1041; *Angew. Chem. Int. Ed.* **2001**, *40*, 988 – 1011; d) N. Sakai, J. Mareda, S. Matile, *Acc. Chem. Res.* **2005**, *38*, 79 – 87; e) T. M. Fyles, *Chem. Soc. Rev.* **2007**, *36*, 335 – 347; f) N. Sakai, Y. Kamikava, M. Nishii, T. Matsuoka, T. Kato, S. Matile, *J. Am. Chem. Soc.* **2006**, *128*, 2218 – 2219.

[7] a) C. Arnal-Hérault, M. Barboiu, A. Pasc, M. Michau, P. Perriat, A. van der Lee, *Chem. Eur. J.* **2007**, *13*, 6792 – 6800; b) R. Custelcean, *Chem. Commun.* **2008**, 295 – 307; c) C. Arnal-Hérault, A. Banu, M. Barboiu, M. Michau, A. van der Lee, *Angew. Chem.* **2007**, *119*, 4346 – 4350; *Angew. Chem. Int. Ed.* **2007**, *46*, 4268 – 4272; d) S. Mihai, A. Cazacu, C. Arnal-Herault, G. Nasr, A. Meffre, A. van der Lee, M. Barboiu, *New J. Chem.* **2009**, *33*, 2335 – 2343; e) S. Mihai, Y. Le Duc, D. Cot, M. Barboiu, *J. Mater. Chem.* **2010**, *20*, 9443 – 9448; f) L. Ma, W. A. Harrell Jr., J. T. Davis, *Org. Lett.* **2009**, *11*, 1599 – 1602; g) M. Barboiu, S. Cerneaux, A. Van der Lee, G. Vaughan, *J. Am. Chem. Soc.* **2004**, *126*, 3545 – 3550; h) M. Barboiu, G. Vaughan, A. Van der Lee, *Org. Lett.* **2003**, *5*, 3073 – 3076; i) A. Cazacu, C. Tong, A. Van der Lee, T. M. Fyles, M. Barboiu, *J. Am. Chem. Soc.* **2006**, *128*, 9541 – 9548; j) A. Cazacu, Y. M. Legrand, A. Pasc, G. Nasr, A. van der Lee, E. Mahon, M. Barboiu, *Proc. Natl. Acad. Sci. USA* **2009**, *106*, 8117 – 8122; k) M. Michau, M. Barboiu, R. Caraballo, C. Arnal-Hérault, P. Periat, A. van der Lee, A. Pasc, *Chem. Eur. J.* **2008**, *14*, 1776 – 1783; l) M. Michau, R. Caraballo, C. Arnal-Hérault, M. Barboiu, *J. Membr. Sci.* **2008**, *321*, 22 – 30; m) M. Michau, M. Barboiu, *J. Mater. Chem.* **2009**, *19*, 6124 – 6131; n) M. Barboiu, *J. Inclusion Phenom. Macrocyclic Chem.* **2004**, *49*, 133 – 137.

[8] a) J. T. Davis, G. P. Spada, *Chem. Soc. Rev.* **2007**, *36*, 296 – 313; b) J. T. Davis, *Angew. Chem.* **2004**, *116*, 684 – 716; *Angew. Chem. Int. Ed.* **2004**, *43*, 668 – 698; c) M. S. Kaucher, W. A. Harrell, J. T. Davis, *J. Am. Chem. Soc.* **2006**, *128*, 38 – 39; d) L. Ma, M. Melegari, M. Colombini, J. T. Davis, *J. Am. Chem. Soc.* **2008**, *130*, 2938 – 2939; e) V. Sidorov, F. W. Koth, G. Abdrakhmanova, R. Mizani, J. C. Fettinger, J. T. Davis, *J. Am. Chem. Soc.* **2002**, *124*, 2267 – 2278; f) C. Arnal-Hérault, A. Pasc-Banu, M. Michau, D. Cot, E. Petit, M. Barboiu, *Angew. Chem.* **2007**, *119*, 8561 – 8565; *Angew. Chem. Int. Ed.* **2007**, *46*, 8409 – 8413; g) C. Arnal-Hérault, M. Barboiu, A. Pasc, M. Michau, P. Perriat, A. van der Lee, *Chem. Eur. J.* **2007**, *13*, 6792 – 6800.

[9] M. Barboiu, *Chem. Commun.* **2010**, *46*, 7466 – 7476.

[10] a) S. Vaitheeeswaran, H. Yin, J. C. Raisaiah, G. Hummer, *Proc. Natl. Acad. Sci. USA* **2004**, *101*, 17002 – 17005; b) L. J. Barbour, G. W. Orr, J. L. Atwood, *Nature* **1998**, *393*, 671 – 673; c) A. Muller, H. Bogge, E. Diemann, *Inorg. Chem. Commun.* **2003**, *6*, 52 – 53; d) M. Yoshizawa, T. Kusukawa, M. Kawano, T. Ohhara, I. Tanaka, K. Kurihara, N. Niimura, M. Fujita, *J. Am. Chem. Soc.* **2005**, *127*, 2798 – 2799.

[11] a) V. Percec, A. E. Dulcey, V. S. K. Balagurusamy, Y. Miura, J. Smirdrkal, M. Peterca, S. Numellin, U. Edlund, S. D. Hudson, P. A. Heiney, H. Duan, S. N. Magonov, S. A. Vinogradov, *Nature* **2004**, *430*, 764 – 768; b) V. Percec, A. E. Dulcey, M. Peterca, M. Ilies, M. J. Sienkowska, P. A. Heiney, *J. Am. Chem. Soc.* **2005**, *127*, 17902 – 17909; c) M. Peterca, V. Percec, A. E. Dulcey, S. Numellin, S. Korey, M. Ilies, P. A. Heiney, *J. Am. Chem. Soc.* **2006**, *128*, 6713 – 6720; d) M. S. Kaucher, M. Peterca, A. E. Dulcey, A. J. Kim, S. A. Vinogradov, D. A. Hammer, P. A. Heiney, V. Percec, *J. Am. Chem. Soc.* **2007**, *129*, 11698 – 11699; e) J. G. Rudick, V. Percec, *Acc. Chem. Res.* **2008**, *41*, 1641 – 1652; f) B. M. Rosen, D. A. Wilson, C. J. Wilson, M. Peterca, B. C. Won, C. Huang, L. R. Lipski, X. Zeng, G. Ungar, P. A. Heiney, V. Percec, *J. Am. Chem. Soc.* **2009**, *131*, 17500 – 17521; g) B. J. Hinds, N. Chopra, R. Andrews, V. Gavalas, L. Bachas, *Science*

2004, *303*, 62 – 65; h) K. Koga, G. T. Gao, H. Tanaka, X. C. Zeng, *Nature* **2001**, *412*, 802 – 805.

[12] a) L. E. Cheruzel, M. S. Pometum, M. R. Cecil, M. S. Mashuta, R. J. Wittebort, R. M. Buchanan, *Angew. Chem.* **2003**, *115*, 5610 – 5613; *Angew. Chem. Int. Ed.* **2003**, *42*, 5452 – 5455; b) Z. Fei, D. Zhao, T. J. Geldbach, R. Scopelliti, P. J. Dyson, S. Antonijevic, G. Bodenhausen, *Angew. Chem.* **2005**, *117*, 5866 – 5871; *Angew. Chem. Int. Ed.* **2005**, *44*, 5720 – 5725; c) Y. M. Legrand, M. Michau, A. van der Lee, M. Barboiu, *CrystEngComm* **2008**, *10*, 490 – 492; d) H. T. Zhang, Y. Z. Li, T. W. Wang, E. N. Nfor, H. Q. Wang, X. Z. You, *Eur. J. Inorg. Chem.* **2006**, 3532 – 3536; e) S. Guha, M. G. B. Drew, A. Banerjee, *Tetrahedron Lett.* **2006**, *47*, 7951 – 7955; f) M. R. Ghadiri, J. R. Granja, L. K. Buehler, *Nature* **1994**, *369*, 301 – 304; g) C. H. Gorbitz, *Chem. Eur. J.* **2007**, *13*, 1022 – 1031; h) U. S. Raghavender, S. Aavinda, N. Shamala, R. Rai, P. Balaram, *J. Am. Chem. Soc.* **2009**, *131*, 15130 – 15132.

[13] In aquaporins water molecules form one H-bond with the protein wall and one with a neighboring water molecule. The opposite orientation of the water molecules along the pore prevents proton transport while permitting rapid water diffusion: E. Tajkhoorshid, P. Nollert, M. O. M. Jensen, L. J. W. Miercke, J. O′Connell, R. M. Stroud, K. Schulten, *Science* **2002**, *296*, 525 – 530.

[14] P. K. Thallapally, G. O. Lloyd, J. L. Atwood, L. J. Barbour, *Angew. Chem.* **2005**, *117*, 2 – 5; *Angew. Chem. Int. Ed.* **2005**, *44*, 2 – 5.

[15] a) L. H. Pinto, G. R. Dieckmann, C. S. Gandhi, C. R. Papworth, J. Braman, M. A. Saughnessy, J. D. Lear, R. A. Lamb, W. F. DeGrado, *Proc. Natl. Acad. Sci. USA* **1997**, *94*, 11301 – 11306; b) S. Phongphanphanee, T. Rungrotmongkol, N. Yoshida, S. Hannongbua, F. Hirata, *J. Am. Chem. Soc.* **2010**, *132*, 9782 – 9788.

[16] J. F. Nagle, H. J. Morowitz, *Proc. Natl. Acad. Sci. USA* **1978**, *75*, 298 – 302.

[17] T. Kar, S. Scheiner, *Int. J. Quantum Chem.* **2006**, *106*, 843 – 851.

[18] M. J. Borgnia, D. Kozano, G. Calamita, P. C. Maloney, P. Agre, *J. Mol. Biol.* **1999**, *291*, 1169 – 1179.

[19] M. Y. Kiriukhin, K. D. Collins, *Biophys. Chem.* **2002**, *99*, 155 – 168.

[20] F. Fornasiero, H. G. Park, J. K. Holt, M. Stadermann, C. P. Grigoropoulos, A. Noy, O. Bakajin, *Proc. Natl. Acad. Sci. USA* **2008**, *105*, 17250 – 17255.

[21] a) B. L. de Groot, H. Grubmueller, *Science* **2001**, *294*, 2353 – 2357; b) Z. Cao, Y. Peng, T. yan, S. Li, A. Li, G. A. Voth, *J. Am. Chem. Soc.* **2010**, *132*, 11395 – 11397.

[22] a) M. C. Burla, M. Camalli, B. Carrozzini, G. L. Cascarano, C. Giacovazzo, G. Polidori, R. Spagna, *J. Appl. Crystallogr.* **2003**, *36*, 1103; b) P. W. Betteridge, J. R. Carruthers, R. I. Cooper, K. Prout, D. J. Watkin, *J. Appl. Crystallogr.* **2003**, *36*, 1487.

